

Scaling Laws for Task-Stratified Knowledge in Post-Training Quantized Large Language Models

Chenxi Zhou^{1,2}, Pengfei Cao^{2,3}, Jiang Li⁴, Jun Zhao^{2,3}, Kang Liu^{2,3*}

¹School of Advanced Interdisciplinary Sciences, University of Chinese Academy of Sciences

²The Key Laboratory of Cognition and Decision Intelligence for Complex Systems, Institute of Automation, Chinese Academy of Sciences

³School of Artificial Intelligence, University of Chinese Academy of Sciences

⁴College of Computer Science, Inner Mongolia University

zhouchenxi2025@ia.ac.cn, {pengfei.cao, jzhao, kliu}@nlpr.ia.ac.cn

Abstract

Large language models (LLMs) present significant deployment challenges due to their scale, with post-training quantization (PTQ) emerging as a practical compression solution. However, a comprehensive understanding of how PTQ precisely impacts diverse LLM knowledge capabilities remains elusive, and existing scaling laws for quantized models often overlook crucial PTQ-specific parameters and task-specific sensitivities. This paper addresses these gaps by conducting an extensive empirical investigation to establish task-stratified scaling laws. We disentangle LLM knowledge into memorization and utilization capabilities and develop a unified quantitative framework that incorporates model size, effective bit-width, calibration set size, and group size. Our central finding reveals that knowledge memorization exhibits markedly greater sensitivity to variations in effective bit-width, calibration set size, and model size compared to the more robust knowledge utilization. These findings offer a fine-grained understanding of PTQ's impact and provide guidance for developing knowledge-aware quantization strategies that can better preserve targeted cognitive functions.

1 Introduction

Large language models (LLMs) have achieved impressive performance across a wide range of tasks (Guo et al., 2023), but their growing scale introduces significant deployment challenges due to high memory and computational costs (Zhu et al., 2024; Lang et al., 2024). Post-training quantization (PTQ) has emerged as a practical and cost-efficient solution to alleviate these challenges by compressing LLMs without expensive retraining (Yao et al., 2023). Importantly, recent study shows that nearly 70% of quantization-related research since 2022 has focused on PTQ for LLMs (Zhao et al., 2025).

Despite the widespread use of PTQ, a comprehensive understanding of how LLM performance is precisely impacted under quantization remains elusive. Current evaluations of quantized LLMs on various benchmarks, while offering general insights like performance cliffs below 4-bit precision (Li et al., 2024) or task-specific sensitivities (Marchisio et al., 2024; Liu et al., 2025), typically lack a systematic and predictive framework. This deficiency makes it difficult for practitioners to make fully informed decisions when configuring PTQ strategies. To this end, some researchers have initiated the exploration of scaling laws for quantized models (Ouyang et al., 2024; Kumar et al., 2025; Xu et al., 2024), aiming to establish relationships between model performance and factors, such as model size or bit-width. Through the scaling laws, the model performance is expected to be predicted after quantization. Nevertheless, existing scaling laws for quantized models still have two notable limitations:

1) How quantization impacts different knowledge capabilities of LLMs is still vague. Current studies mainly focus on investigating the overall performance of the quantized LLMs, but lack a deep dive into how these capabilities are individually affected. This oversight is critical, as LLMs possess diverse abilities like knowledge memorization (recalling factual information) and knowledge utilization (applying knowledge for reasoning and problem-solving) (Wang et al., 2024; Yu et al., 2024). These distinct functions or capabilities, likely due to their different operational mechanisms, are hypothesized to respond variably to quantization. Therefore, task-stratified scaling laws are needed to capture these nuanced sensitivities and guide PTQ strategies to preserve targeted abilities.

2) The scope of quantization variables considered in current scaling laws is incomplete.

*Corresponding Author

Existing works on PTQ scaling laws predominantly focused on factors like model size, bit-width and training data. However, crucial PTQ-specific tunable factors, which significantly influence the final performance of quantized models, such as calibration set size (Zhang et al., 2025) and group size (Elangovan et al., 2025) (which are integral to widely used methods like GPTQ (Frantar et al., 2023), AWQ (Lin et al., 2024), and SmoothQuant (Xiao et al., 2023)) are usually overlooked. The omission of these factors when investigating scaling laws will cause a “granularity gap”, which limits the practical guidance these laws can offer for configuring optimal PTQ strategies.

To address the aforementioned limitations, the paper conducts an extensive empirical investigation to establish **Task-Stratified Knowledge Scaling Laws** for post-training quantized LLMs. Our fine-grained analysis involves: 1) *Systematically investigating how PTQ impacts LLM knowledge capabilities (knowledge memorization and knowledge utilization)*. 2) *Comprehensively incorporating model size, bit-width, calibration set size, and group size into a unified quantitative framework based on multiplicative power laws*. From 384 unique PTQ configurations, our central finding is that: **knowledge memorization exhibits markedly greater sensitivity to variations in effective bit-width, calibration set size and model size compared to knowledge utilization**. This finding has significant implications for optimizing quantized LLMs.

In summary, the contributions are threefold. **Firstly**, we introduce and empirically validate the first task-stratified PTQ scaling laws that reveal the capabilities of LLM knowledge memorization and utilization have distinct sensitivities to quantization configurations. **Secondly**, we address a critical “granularity gap” by systematically incorporating model size, effective bit-width, alongside crucial PTQ-specific parameters (calibration set size and group size) into a unified power-law scaling framework. **Thirdly**, A data-driven guidance for knowledge-aware quantization is given based on the central finding in the paper, that knowledge memorization exhibits markedly higher sensitivity than knowledge utilization to variations in model size, effective bit-width, and calibration set size.

2 Related Work

2.1 Post-Training Quantization of LLMs

Post-Training Quantization (PTQ) has become a mainstream approach for LLM compression due to its efficiency and lower resource requirements. Unlike Quantization-Aware Training (QAT), which requires extensive retraining, PTQ operates directly on pre-trained models (Lang et al., 2024; Hasan, 2024). While PTQ is straightforward to implement, it can potentially degrade model accuracy, thereby requiring careful calibration to balance compression ratios and performance (Williams and Aletras, 2024; Ji et al., 2024).

There is a wide variety of PTQ methods. Among them, GPTQ is a pioneering compensation-based PTQ method. It utilizes Hessian matrix to reconstruct quantization errors and updates the remaining unquantized weights after quantizing specific weights to minimize the impact on model output (Frantar et al., 2023). The widespread application of PTQ (Zhao et al., 2025) making it a suitable benchmark method in our study.

2.2 Scaling Laws for Quantized LLMs

Neural scaling laws offer a foundational framework for understanding how the performance of LLMs varies with key factors such as model size, dataset size, and training compute. Pioneering work by Kaplan et al. (2020) demonstrates that the performance of uncompressed LLMs typically improves as power laws of these factors, establishing that “scale is key”. Subsequently, Hoffmann et al. (2022) further refine these insights with the Chinchilla scaling laws, proposing that for compute-optimal training, model size and training dataset size should scale in roughly equal proportion.

Researchers have subsequently begun to explore scaling laws specifically for quantized LLMs (Ouyang et al., 2024; Kumar et al., 2025; Frantar et al., 2025). For instance, Ouyang et al. (2024) investigate scaling laws for quantization-induced degradation (QiD), linking QiD to training data volume, model size, and bit-width. Kumar et al. (2025) explore the interplay between training precision and PTQ precision. Sun et al. (2025) study scaling laws for floating-point quantization training, considering exponent bits, mantissa bits, and group size. Furthermore, Xu et al. (2024) highlight the unpredictability of post-PTQ model quality and attempt to build predictive models considering various factors. Despite advancements in scaling laws

for compressed models, there’s a lack of in-depth research into their effects on distinct knowledge capabilities and a comprehensive consideration of quantization factors, which hinders practical application guidance. Consequently, our work explores scaling laws for the knowledge capabilities of quantized models.

3 Task-Stratified Knowledge Scaling Laws for PTQ LLMs

3.1 Task Capability Definitions for Quantization Analysis

To comprehensively investigate the impact of PTQ on LLMs, we distinguish between two core knowledge capabilities: **Knowledge Memorization** and **Knowledge Utilization**. This differentiation is crucial, as these capabilities are hypothesized to depend on distinct underlying neural mechanisms (Zheng et al., 2024; Wang et al., 2024), consequently, may exhibit varying degrees of sensitivity to PTQ. Understanding these distinct sensitivities is key to developing task-stratified scaling laws and targeted quantization strategies.

(1) Knowledge Memorization (KM) refers to an LLM’s ability to accurately recall factual information, associative knowledge, and specific details learned during its pre-training phase. This capability is characterized by its reliance on the direct recall of explicit, often discrete, pieces of knowledge. KM is typically evaluated using tasks that directly probe this recall ability, such as cloze-style questioning where the model must identify missing entities in factual statements (e.g., LAMA (Petroni et al., 2019)), or tasks requiring statement verification against an established corpus of facts to assess factual accuracy (e.g., TruthfulQA (Lin et al., 2022)). Performance on such tasks directly indicates the model’s capacity to preserve its precise internal knowledge base after quantization.

(2) Knowledge Utilization (KU), in contrast, encompasses an LLM’s ability to leverage its learned knowledge for complex cognitive operations that extend beyond simple recall. This requires the model to reason, make inferences, understand context, and solve problems, often in novel scenarios. Key characteristics of KU include the manipulation, integration, and flexible deployment of internalized knowledge. This capability is typically assessed using benchmarks targeting commonsense reasoning (e.g., Hellaswag (Zellers et al., 2019); Winogrande (SakaguchiKeisuke et al., 2021)), read-

ing comprehension demanding inferential steps, or multi-step problem-solving (e.g., ARC (Clark et al., 2018)). Quantization’s impact on these tasks reveals the extent to which the model retains its ability to generalize and effectively deploy its knowledge in dynamic contexts.

The core distinction lies in cognitive demand: KM emphasizes information fidelity, while KU focuses on the effective utilization and generalization of that information. Our empirically motivated separate evaluation of these capabilities aims to construct distinct scaling laws, predicting how PTQ configurations differentially affect factual recall versus broader reasoning abilities for more informed model optimization.

3.2 Factors under Investigation

To develop comprehensive task-stratified scaling laws for PTQ LLMs, we identify and analyze a set of key factors.

(1) Model Size (N): Defined as the total number of parameters in an LLM, model size is a foundational determinant of its capabilities. Larger models generally possess greater representational capacity and may exhibit varying degrees of robustness to quantization noise (Badshah and Sajjad, 2024; Marchisio et al., 2024). While established scaling laws for uncompressed models indicate a power-law relationship between model size and performance (Kaplan et al., 2020; Hoffmann et al., 2022), a core component of our investigation is to determine how this relationship is modulated by PTQ parameters and whether it holds consistently across different knowledge capabilities in quantized models.

(2) Calibration Set Size (C_b): Represents the number of samples used during the PTQ calibration phase, which are essential for methods like GPTQ to estimate quantization parameters by minimizing reconstruction error. While the general importance of calibration data is acknowledged (Zhang et al., 2025; Williams and Aletras, 2024; Ji et al., 2024), its systematic scaling behavior, particularly its interplay with other PTQ parameters and differential impact on distinct knowledge capabilities, remains under-explored in existing scaling laws.

As illustrated in Figure 1, C_b can exert a substantial influence on the quantized model’s accuracy. Notably, increasing C_b yields considerable performance gains, especially at lower bit-widths, though typically with diminishing returns. This observed sensitivity and non-linear impact motivate its inclu-

sion as a key factor in our task-stratified scaling laws, aiming to quantify its contribution to preserving different types of knowledge.

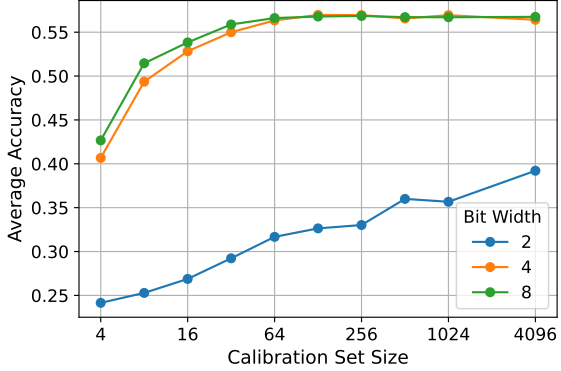


Figure 1: Average accuracy over four downstream datasets (Lambda, WinoG., ARC-e, ARC-c) for the OPT-6.7B model as a function of C_b under different GPTQ quantization ($G = 128$).

(3) Group Size (G): In many advanced PTQ methods like GPTQ, weights are quantized in groups rather than individually to achieve a better trade-off between accuracy and efficiency. It is a key tunable parameter that determines the granularity of error compensation; smaller groups allow for more fine-grained adjustments but may increase metadata overhead and computational cost (Frantar et al., 2023; Elangovan et al., 2025). Figure 2 compellingly illustrates the critical role of G , particularly at low bit-widths where smaller group sizes (e.g., 32, 64) lead to substantially better average accuracy, with performance degrading as G increases.

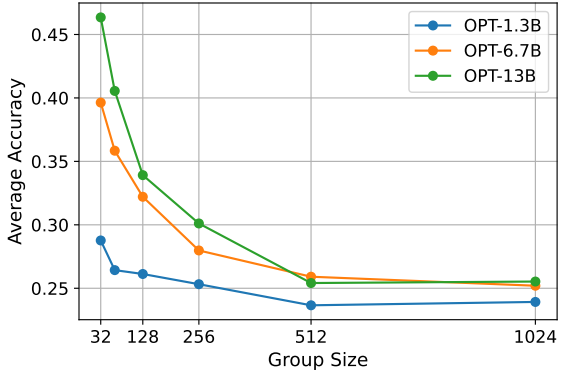


Figure 2: Average accuracy over four downstream tasks (Lambda, WinoG., ARC-e, ARC-c) for OPT models of varying sizes as a function of group size under 2-bit GPTQ quantization ($C_b = 128$).

(4) Effective Bit-width (B_{eff}): Nominal bit-width (W_{base}), such as 2, 3, 4, or 8 bits, typically

only reflects the precision of the quantized weights themselves. However, to accurately assess the true information density per parameter in prevalent PTQ methods, particularly those employing grouped quantization like GPTQ (Frantar et al., 2023), we introduce the concept of effective bit-width (B_{eff}). This metric accounts for the additional storage overhead from metadata, including scale factors and zero-points, which is essential for dequantization but is shared across a group of weights (Elangovan et al., 2025). We define B_{eff} as follows:

$$B_{eff} = W_{base} + \frac{b_s + b_z}{G} \quad (1)$$

where W_{base} represents the nominal bit-width for the quantized weights (e.g., 2, 3, 4 bits). b_s is the bit-width for storing the scale factor for each group of weights. In our study, b_s is consistently set to 16 bits (representing FP16 precision), a common choice to maintain accuracy during dequantization. b_z denotes the bit-width for storing the zero-point for each group. For asymmetric quantization schemes, we assume $b_z = W_{base}$. For perfectly symmetric quantization schemes, b_z would be 0.

This formulation of B_{eff} offers a more faithful representation of the actual information density and compression cost per parameter. The significance of B_{eff} as a critical factor influencing model performance is illustrated in Figure 3, which shows a clear trend between average accuracy and varying effective bit-widths across different OPT model sizes. This underscores the necessity of considering B_{eff} rather than nominal bit-width alone in our scaling law analysis.

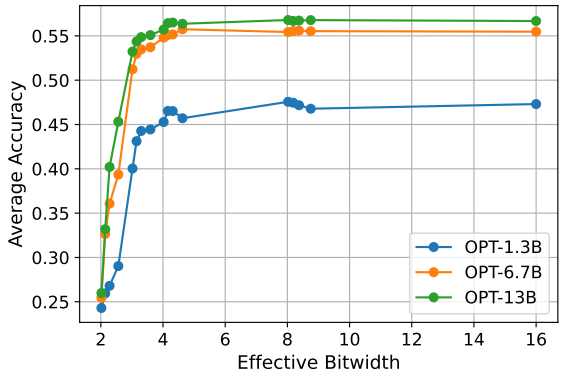


Figure 3: Impact of B_{eff} on the average accuracy of OPT models over five datasets (Lambda, HellaS., WinoG., ARC-e, and ARC-c), with $C_b = 128$.

3.3 Scaling Law Formulation and Fitting Procedure

This section details the formulation of our task-stratified scaling laws and the methodology for their empirical fitting.

3.3.1 Functional Form of the Task-Stratified Scaling Law

The performance is denoted as Acc_{task} , on a specific knowledge capability type (KM / KU), which can be modeled as a multiplicative power-law function of the key PTQ factors:

$$Acc_{task} \approx C_{task} \times N^{\alpha_{task}} \times [\log_2(C_b)]^{\beta_{task}} \times G^{\gamma_{task}} \times [\log_2(B_{eff})]^{\delta_{task}}, \quad (2)$$

where C_{task} is a task-specific constant scaling coefficient. N , C_b , G , and B_{eff} represent the model size, calibration set size, group size, and effective bit-width, respectively, as previously defined. The exponents α_{task} , β_{task} , γ_{task} , δ_{task} are task-specific scaling parameters, quantifying the sensitivity of performance on that task type to each respective factor.

The adoption of a multiplicative power-law form is motivated by its established success in describing scaling phenomena in LLMs, where model parameters and performance metrics often exhibit such relationships (Kaplan et al., 2020; Hoffmann et al., 2022). This functional form also allows the exponents to be interpreted directly as elasticities, indicating the proportional change in accuracy resulting from a proportional change in a given factor.

3.3.2 Rationale for Logarithmic Transformation of C_b and B_{eff}

The terms for C_b and B_{eff} in our scaling law (i.e., Eq.(2)) are logarithmically transformed (\log_2). This approach is adopted to effectively model the non-linear relationship these factors exhibit with model accuracy, characterized by diminishing returns. Specifically, initial increases in C_b or B_{eff} tend to yield substantial performance gains, but these gains progressively lessen as the values of these parameters become larger.

This diminishing returns phenomenon is empirically supported by our experiments. For instance, Figure 1 illustrates that while larger calibration sets generally improve accuracy, particularly at lower bit-widths, the improvement saturates at higher C_b

values. Similarly, Figure 3 shows that increasing B_{eff} boosts performance, but the rate of improvement diminishes as B_{eff} increases. The logarithmic terms $\log_2(C_b)$ and $\log_2(B_{eff})$ are thus crucial for capturing these observed saturation effects and ensuring our scaling laws accurately reflect performance across diverse PTQ configurations. This aligns with prior work suggesting that the utility of additional calibration data (Williams and Aletras, 2024) and increased bit-width (Li et al., 2024) often follows such a non-linear pattern.

3.3.3 Fitting Procedure

The parameters of our task-stratified scaling law, namely the task-specific constant (C_{task}) and exponents (γ_{task} , α_{task} , β_{task} , δ_{task}), are estimated by fitting the model to the empirical data collected across different configurations of N , G , C_b , and B_{eff} .

To robustly estimate parameters for Eq. (2), especially with potentially low accuracy scores, we employ direct non-linear least squares (NLS) regression (Amemiya, 1983). This method fits the power law directly to untransformed Acc_{task} data, avoiding issues with log-transforming low accuracies common in traditional Ordinary Least Squares (OLS) fitting of linearized power laws (Sengupta et al., 2025). We perform NLS fitting using SciPy’s `curve_fit` function¹. Goodness of fit is primarily assessed using the adjusted R^2 statistic (details in Appendix C), calculated on the original accuracy scale.

4 Experiments and Results

4.1 Experimental Setup

We design a comprehensive experimental setup to evaluate how key PTQ parameters affect distinct LLM knowledge capabilities. Our primary investigation utilize the GPTQ method (Frantar et al., 2023) on the OPT model family (Zhang et al., 2022). We systematically vary model size (N – 6 variants from 125M to 13B), nominal weight bit-width (W_{base} – 4 variants), calibration set size (C_b – 4 variants), and group size (G – 4 variants). This approach ($6 \times 4 \times 4 \times 4$) resulted in **384 unique PTQ configurations**. Standard calibration datasets were used, avoiding overlap with evaluation benchmarks. Performance was assessed in a zero-shot setting for knowledge memorization and utilization. Further experimental details are provided in

¹<https://scipy.org/>

Appendix A.

4.2 General Scaling Law for Overall Knowledge Capability

To understand the collective impact of PTQ parameters on overall LLM knowledge capabilities, we first derive a general scaling law. This law models $Acc_{general}$, an aggregated accuracy across our six downstream tasks (covering knowledge memorization and utilization) for OPT models quantized with GPTQ. Adopting the functional form of Eq. (2), $Acc_{general}$ is modeled as: $Acc_{general} \approx C \times N^\alpha \times [\log_2(C_b)]^\beta \times G^\gamma \times [\log_2(B_{eff})]^\delta$. The parameters ($C, \alpha, \beta, \gamma, \delta$) are fitted to the $Acc_{general}$ data to capture broad performance trends before we analyze task-specific sensitivities.

4.2.1 Analysis of PTQ Factors

To elucidate the individual and combined importance of the four key factors—model size (N), effective bit-width (B_{eff}), calibration set size (C_b), and group size (G)—on general model performance, we conduct an ablation study. We fit variants of Eq. (2) with different combinations of these factors, evaluating the goodness-of-fit using the Adjusted R^2 statistic. The results shown in Table 1 and Figure 4 reveal several key insights regarding factor importance:

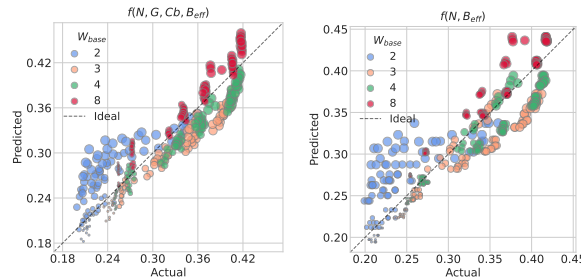


Figure 4: Goodness-of-fit for the baseline scaling law: predicted vs. actual average task accuracy. (Left): Four-variable model ($f(N, G, C_b, B_{eff})$). (Right): Two-variable model ($f(N, B_{eff})$). Point color indicates base weight bit-width and size corresponds to model size. The dashed line represents ideal prediction ($y=x$).

(1) Comprehensive four-factor model achieves highest goodness-of-fit: The full four-variable model ($Acc = f(N, C_b, G, B_{eff})$) yields the highest Adjusted R^2 of 0.8319 across our 384 unique PTQ configurations, indicating a good overall model fit. Figure 4 (left) provides visual support for this observation; empirical data points are generally

distributed along the $y = x$ diagonal, and this correspondence across different base bit-widths and model sizes suggests effective predictive capability. This outcome underscores the importance of a comprehensive, fine-grained parameterization for modeling the behavior of quantized LLMs.

(2) Key contributions of N and B_{eff} : The strong fit of the comprehensive model is largely attributable to the key contributions of N and B_{eff} . A simpler model incorporating only these two factors ($Acc = f(N, B_{eff})$) yields a substantial adjusted R^2 of 0.8024. Their positive scaling exponents ($\alpha \approx 0.1011, \delta \approx 0.3211$) confirm that larger capacity and higher effective precision are beneficial. However, as shown in Figure 4 (right), the predictions from this two-variable model exhibit noticeably greater scatter around the ideal $y = x$ line compared to the four-variable model, indicating that while N and B_{eff} are dominant, they alone do not capture the full performance variation.

(3) C_b as an Important Factor for Model Fit: Introducing C_b to the (N, B_{eff}) model notably increases the Adjusted R^2 to 0.8319, a level of fit comparable to that of the full four-factor model. This highlights C_b as a critical determinant, with its positive exponent ($\beta \approx 0.0705$) validating the importance of sufficient calibration data.

(4) Nuanced Role of G : The direct inclusion of group size (G) into the aggregate model shows a more subtle effect on the adjusted R^2 . Adding G to the (N, B_{eff}) model does not improve upon the simpler two-variable fit. Moreover, its fitted exponent γ in the full model is very small (-0.0035). This suggests that G 's primary influence on accuracy is largely mediated through its impact on B_{eff} . The G^γ term in the full model likely captures residual granularity effects.

Figure 5 visually confirms the efficacy and predictive power of our four-variable baseline scaling law across various PTQ configurations. The subplots consistently show accurate trend capture for quantized OPT models under different G and C_b settings. Furthermore, the figure illustrates how the scaling law correctly predicts increased accuracy with larger N and higher B_{eff} , and demonstrates the positive influence of larger C_b and smaller G values. These visual trends align well with the quantitative findings in Table 1, affirming the robustness of our general PTQ performance model.

Form	Fitted Function	Adj. R^2
$Acc = f(N, C_b, G, B_{eff})$	$Acc \approx 0.0255 \times N^{0.1016} \times [\log_2(C_b)]^{0.0706} \times G^{-0.0035} \times [\log_2(B_{eff})]^{0.3188}$	0.8319
$Acc = f(N, B_{eff})$	$Acc \approx 0.0291 \times N^{0.1011} \times [\log_2(B_{eff})]^{0.3211}$	0.8024
$Acc = f(N, G, B_{eff})$	$Acc \approx 0.0295 \times N^{0.1012} \times G^{-0.0034} [\log_2(B_{eff})]^{0.3198}$	0.8023
$Acc = f(N, C_b, B_{eff})$	$Acc \approx 0.0251 \times N^{0.1015} \times [\log_2(C_b)]^{0.0705} \times [\log_2(B_{eff})]^{0.3201}$	0.8319

Table 1: Fitted scaling laws for the overall 6-task average accuracy (Acc) of quantized LLMs using different variable combinations. The adjusted R^2 values indicate the goodness-of-fit for each functional form, highlighting the necessity of factors we considered.

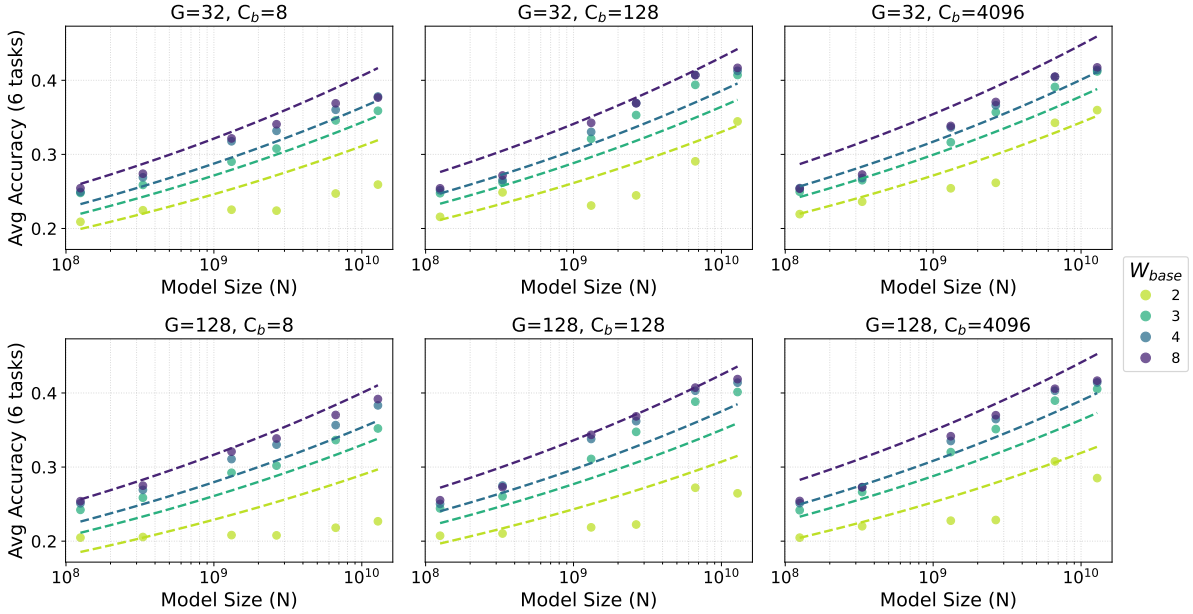


Figure 5: Empirical data (point) and fitted general scaling law (dashed lines) for average accuracy on 6 tasks. Subplots show performance varying with N under different W_{base} , for 6 fixed combinations of different G and C_b .

4.2.2 Parameter Sensitivity in Low-Bit Regimes

While the overall four-variable model offers a valuable general overview, its parameters reflect average effects across a wide range of bit-widths. In aggressive low-bit quantization regimes, however, sensitivity to certain PTQ parameters, notably G and C_b , becomes markedly more pronounced. The specific impacts in these scenarios, particularly for 2-bit GPTQ quantization as illustrated by the fitted surfaces in Figure 7, are summarized below.

Pronounced Sensitivity to C_b and G at 2-bit Precision. (1) Larger C_b values consistently improve accuracy across different model sizes (N) and group size (G). (2) Smaller G values yield markedly better accuracy. This heightened influence of G at 2-bit precision, evidenced by a large negative exponent (-0.0904) in its specific scaling

fit, underscores its critical role in aggressive quantization, contrasting with its more subtle role in the general model.

Contextualizing the Role of Group Size (G) in the General Model. The diminished direct impact of G in the general model (exponent -0.0035) compared to its pronounced effect at 2-bit precision (-0.0904) is primarily because: (1) the B_{eff} term in the general model already incorporates a significant portion of the effect of G on precision, and (2) the general model averages performance across diverse bit-widths (2-bit to 8-bit), thus masking the heightened importance of G at very low bit-widths. Therefore, despite a modest direct coefficient in the general scaling law, G retains substantial practical importance in low-precision deployments..

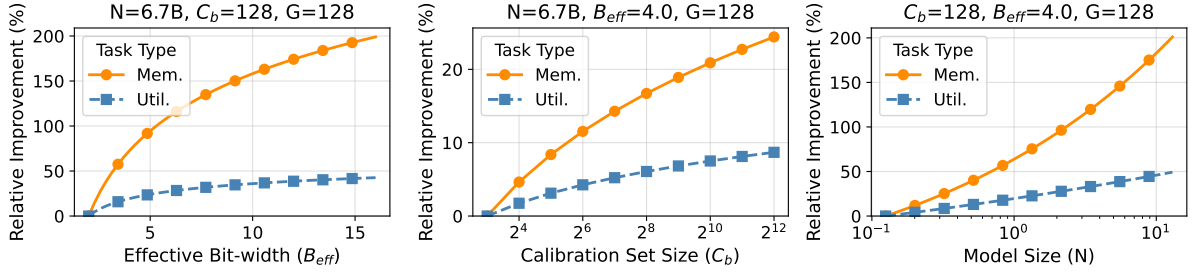


Figure 6: Relative performance improvement (%) for two tasks, as predicted by their respective scaling laws. The performance varied with B_{eff} , C_b , and N , while other parameters are held at representative baseline values.

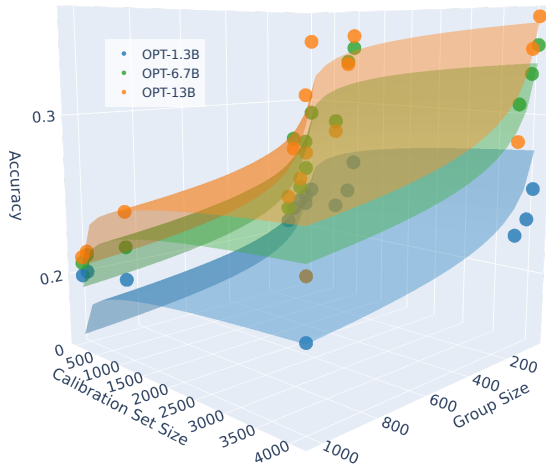


Figure 7: Fitted scaling surfaces illustrating the combined impact of N , G , and C_b on average task accuracy under 2-bit quantization. Points represent empirical data. The surfaces are derived from a 3-variable fit specific to the 2-bit scenario ($\text{Accuracy} \approx 2.4915 \times 10^{-2} \cdot N^{0.1085} \cdot G^{-0.0904} \cdot [\log_2(C_b)]^{0.1748}$, $R^2 = 0.8828$).

4.3 Task-Stratified Scaling Laws: Memorization vs. Utilization

While the baseline scaling law (Section 4.2) provides a general overview, it averages out distinct sensitivities across different cognitive capabilities. To dissect these, we derive separate scaling laws for Knowledge Memorization (Acc_{mem}) and Knowledge Utilization (Acc_{util}), fitting them independently to their respective benchmark data. Table 2 details these fitted parameters alongside the general law. Our analysis yields two primary findings.

Firstly, our task-stratified scaling laws effectively model performance for distinct knowledge capabilities. KU shows a strong fit ($\text{Adj. } R^2 \approx 0.84$), comparable to the general model. KM also demonstrates a substantial fit ($\text{Adj. } R^2 \approx 0.75$); its slightly lower value might indicate higher inherent variability or sensitivity to subtle quantization effects not fully captured by the examined macro-

Tasks	C	$\alpha(N)$	$\beta(C_b)$	$\gamma(G)$	$\delta(B_{eff})$	Adj. R^2
General	2.55×10^{-2}	0.1016	0.0706	-0.0035	0.3188	0.83
Mem.	2.37×10^{-4}	0.2373	0.1576	-0.0036	0.7900	0.75
Util.	5.13×10^{-2}	0.0862	0.0601	-0.0036	0.2561	0.84

Table 2: Fitted parameters of $Acc \approx C \times N^\alpha \times [\log_2(C_b)]^\beta \times G^\gamma \times [\log_2(B_{eff})]^\delta$ on OPT model family.

scopic parameters, a notion visually supported by the distinct trend patterns observed in Figure 6.

Secondly, and more critically, Knowledge Memorization exhibits markedly higher sensitivity to PTQ configurations than Knowledge Utilization. This is evidenced by: (1) *Quantitative Disparities*: Table 2 shows KM’s scaling exponents for key parameters—model size (N), effective bit-width (B_{eff}), and calibration set size (C_b)—are substantially larger than KU’s. (2) *Visual Confirmation*: Figure 6 visually corroborates this with steeper performance improvement trends for KM concerning these parameters. This combined evidence indicates KM tasks are inherently more “fragile” under quantization, heavily depending on numerical precision, model capacity, and calibration, while KU tasks show greater robustness.

5 Conclusion

This paper introduces and empirically validates task-stratified PTQ scaling laws, demonstrating how LLM performance on distinct knowledge memorization and utilization tasks scales with model size, effective bit-width, calibration set size, and group size. Our central finding reveals that knowledge memorization exhibits markedly greater sensitivity to variations in N , B_{eff} , and C_b compared to the more robust knowledge utilization, a difference quantitatively supported by their distinct scaling exponents. This framework addresses a significant “granularity gap” in prior scaling literature by comprehensively integrating

these fine-grained PTQ parameters. It thereby offers an empirically-backed foundation for developing knowledge-aware PTQ strategies, with the generalizability of these insights supported by experiments on architectures like LLaMA2.

Limitations

While this work establishes foundational task-stratified PTQ scaling laws, we identify areas for future exploration. Our study primarily focused on prevalent transformer architectures (OPT, LLaMA2) and weight-only PTQ (specifically GPTQ). Future work could extend this framework to newer architectures and a broader range of quantization methods, including activation quantization, potentially requiring adjustments to the scaling law formulations. Additionally, our current knowledge stratification (memorization vs. utilization) is an initial step; investigating a more diverse set of complex cognitive tasks and benchmarks would provide deeper insights into PTQ’s nuanced impacts on the multifaceted capabilities of LLMs.

References

Takeshi Amemiya. 1983. Non-linear regression models. *Handbook of econometrics*, 1:333–389.

Sher Badshah and Hassan Sajjad. 2024. Quantifying the Capabilities of LLMs across Scale and Precision. *arXiv preprint*. ArXiv:2405.03146.

Peter Clark, Isaac Cowhey, Oren Etzioni, Tushar Khot, Ashish Sabharwal, Carissa Schoenick, and Oyvind Tafjord. 2018. Think you have Solved Question Answering? Try ARC, the AI2 Reasoning Challenge. *arXiv preprint*. ArXiv:1803.05457.

AutoGPTQ contributors. 2024. Autogptq.

Reena Elangovan, Charbel Sakr, Anand Raghunathan, and Brucek Khailany. 2025. BCQ: Block Clustered Quantization for 4-bit (W4A4) LLM Inference. *arXiv preprint*. ArXiv:2502.05376.

Elias Frantar, Saleh Ashkboos, Torsten Hoefer, and Dan Alistarh. 2023. GPTQ: Accurate Post-Training Quantization for Generative Pre-trained Transformers. *arXiv*. ArXiv:2210.17323.

Elias Frantar, Utku Evcı, Wonpyo Park, Neil Houlsby, and Dan Alistarh. 2025. Compression Scaling Laws: Unifying Sparsity and Quantization. *arXiv preprint*.

Zishan Guo, Renren Jin, Chuang Liu, Yufei Huang, Dan Shi, Supryadi, Linhao Yu, Yan Liu, Jiaxuan Li, Bojian Xiong, and Deyi Xiong. 2023. Evaluating Large Language Models: A Comprehensive Survey. *arXiv preprint*. ArXiv:2310.19736.

Jahid Hasan. 2024. Optimizing Large Language Models through Quantization: A Comparative Analysis of PTQ and QAT Techniques. *arXiv preprint*.

Jordan Hoffmann, Sebastian Borgeaud, Arthur Mensch, Elena Buchatskaya, Trevor Cai, Eliza Rutherford, Diego de Las Casas, Lisa Anne Hendricks, Johannes Welbl, Aidan Clark, Tom Hennigan, Eric Noland, Katie Millican, George van den Driessche, Bogdan Damoc, Aurelia Guy, Simon Osindero, Karen Simonyan, Erich Elsen, and 3 others. 2022. Training Compute-Optimal Large Language Models. *arXiv preprint*. ArXiv:2203.15556.

Yixin Ji, Yang Xiang, Juntao Li, Qingrong Xia, Ping Li, Xinyu Duan, Zhefeng Wang, and Min Zhang. 2024. Beware of Calibration Data for Pruning Large Language Models. *arXiv preprint*. ArXiv:2410.17711.

Jared Kaplan, Sam McCandlish, Tom Henighan, Tom B. Brown, Benjamin Chess, Rewon Child, Scott Gray, Alec Radford, Jeffrey Wu, and Dario Amodei. 2020. Scaling Laws for Neural Language Models. *arXiv preprint*. ArXiv:2001.08361.

Tanishq Kumar, Zachary Ankner, Benjamin F. Spector, Blake Bordelon, Niklas Muennighoff, Mansheej Paul, Cengiz Pehlevan, Christopher Ré, and Aditi Raghunathan. 2025. Scaling Laws for Precision. *arXiv*.

Jiedong Lang, Zhehao Guo, and Shuyu Huang. 2024. A Comprehensive Study on Quantization Techniques for Large Language Models. *arXiv preprint*. ArXiv:2411.02530.

Shiying Li, Xuefei Ning, Luning Wang, Tengxuan Liu, Xiangsheng Shi, Shengen Yan, Guohao Dai, Huazhong Yang, and Yu Wang. 2024. Evaluating Quantized Large Language Models. *arXiv*.

Ji Lin, Jiaming Tang, Haotian Tang, Shang Yang, Wei-Ming Chen, Wei-Chen Wang, Guangxuan Xiao, Xingyu Dang, Chuang Gan, and Song Han. 2024. AWQ: Activation-aware Weight Quantization for On-Device LLM Compression and Acceleration. *Proceedings of Machine Learning and Systems*, 6:87–100.

Stephanie Lin, Jacob Hilton, and Owain Evans. 2022. TruthfulQA: Measuring How Models Mimic Human Falsehoods. *arXiv preprint*. ArXiv:2109.07958.

Ruikang Liu, Yuxuan Sun, Manyi Zhang, Haoli Bai, Xianzhi Yu, Tiezheng Yu, Chun Yuan, and Lu Hou. 2025. Quantization Hurts Reasoning? An Empirical Study on Quantized Reasoning Models. *arXiv preprint*. ArXiv:2504.04823.

Kelly Marchisio, Saurabh Dash, Hongyu Chen, Dennis Aumiller, Ahmet Üstün, Sara Hooker, and Sebastian Ruder. 2024. How Does Quantization Affect Multilingual LLMs? In *Findings of the Association for Computational Linguistics: EMNLP 2024*, pages 15928–15947, Miami, Florida, USA. Association for Computational Linguistics. 250116 rate: 5.

Stephen Merity, Caiming Xiong, James Bradbury, and Richard Socher. 2016. **Pointer Sentinel Mixture Models**. *arXiv preprint*. ArXiv:1609.07843.

Xu Ouyang, Tao Ge, Thomas Hartvigsen, Zhisong Zhang, Haitao Mi, and Dong Yu. 2024. **Low-Bit Quantization Favors Undertrained LLMs: Scaling Laws for Quantized LLMs with 100T Training Tokens**. *arXiv preprint*.

Fabio Petroni, Tim Rocktäschel, Sebastian Riedel, Patrick Lewis, Anton Bakhtin, Yuxiang Wu, and Alexander Miller. 2019. **Language Models as Knowledge Bases?** In *Proceedings of the 2019 Conference on Empirical Methods in Natural Language Processing and the 9th International Joint Conference on Natural Language Processing (EMNLP-IJCNLP)*, pages 2463–2473, Hong Kong, China. Association for Computational Linguistics.

SakaguchiKeisuke, BrasRonan Le, BhagavatulaChandra, and ChoiYejin. 2021. **WinoGrande**. *Communications of the ACM*. Publisher: ACMPUB27New York, NY, USA.

Ayan Sengupta, Siddhant Chaudhary, and Tanmoy Chakraborty. 2025. **Compression Laws for Large Language Models**. *arXiv preprint*.

Xingwu Sun, Shuaipeng Li, Ruobing Xie, Weidong Han, Kan Wu, Zhen Yang, Yixing Li, An Wang, Shuai Li, Jinbao Xue, Yu Cheng, Yangyu Tao, Zhanhui Kang, Chengzhong Xu, Di Wang, and Jie Jiang. 2025. **Scaling Laws for Floating Point Quantization Training**. *arXiv*. ArXiv:2501.02423.

Hugo Touvron, Louis Martin, Kevin Stone, Peter Albert, Amjad Almahairi, Yasmine Babaei, Nikolay Bashlykov, Soumya Batra, Prajwal Bhargava, Shruti Bhosale, Dan Bikel, Lukas Blecher, Cristian Canton Ferrer, Moya Chen, Guillem Cucurull, David Esiobu, Jude Fernandes, Jeremy Fu, Wenyin Fu, and 49 others. 2023. **Llama 2: Open Foundation and Fine-Tuned Chat Models**. *arXiv preprint*. ArXiv:2307.09288.

Mengru Wang, Yunzhi Yao, Ziwen Xu, Shuofei Qiao, Shumin Deng, Peng Wang, Xiang Chen, Jia-Chen Gu, Yong Jiang, Pengjun Xie, Fei Huang, Huajun Chen, and Ningyu Zhang. 2024. **Knowledge Mechanisms in Large Language Models: A Survey and Perspective**. *arXiv*.

Miles Williams and Nikolaos Aletras. 2024. **On the Impact of Calibration Data in Post-training Quantization and Pruning**. *ArXiv*:2311.09755.

Thomas Wolf, Lysandre Debut, Victor Sanh, Julien Chaumond, Clement Delangue, Anthony Moi, Pieric Cistac, Tim Rault, Remi Louf, Morgan Funtowicz, Joe Davison, Sam Shleifer, Patrick von Platen, Clara Ma, Yacine Jernite, Julien Plu, Canwen Xu, Teven Le Scao, Sylvain Gugger, and 3 others. 2020. **Transformers: State-of-the-Art Natural Language Processing**. In *Proceedings of the 2020 Conference on Empirical Methods in Natural Language Processing*: System Demonstrations, pages 38–45, Online. Association for Computational Linguistics.

Guangxuan Xiao, Ji Lin, Mickael Seznec, Hao Wu, Julien Demouth, and Song Han. 2023. **SmoothQuant: Accurate and Efficient Post-Training Quantization for Large Language Models**. In *Proceedings of the 40th International Conference on Machine Learning*, pages 38087–38099. PMLR. ISSN: 2640-3498.

Zifei Xu, Alexander Lan, Wanzin Yazar, Tristan Webb, Sayeh Sharify, and Xin Wang. 2024. **Scaling Laws for Post Training Quantized Large Language Models**. *arXiv preprint*.

Zhewei Yao, Xiaoxia Wu, Cheng Li, Stephen Youn, and Yuxiong He. 2023. **A Comprehensive Study on Post-Training Quantization for Large Language Models**. *arXiv preprint*.

Jifan Yu, Xiaozhi Wang, Shangqing Tu, Shulin Cao, Daniel Zhang-Li, Xin Lv, Hao Peng, Zijun Yao, Xiaohan Zhang, Hanming Li, Chunyang Li, Zheyuan Zhang, Yushi Bai, Yantao Liu, Amy Xin, Nianyi Lin, Kaifeng Yun, Linlu Gong, Jianhui Chen, and 16 others. 2024. **KoLA: Carefully Benchmarking World Knowledge of Large Language Models**. *arXiv*.

Rowan Zellers, Ari Holtzman, Yonatan Bisk, Ali Farhadi, and Yejin Choi. 2019. **HellaSwag: Can a Machine Really Finish Your Sentence?** *arXiv preprint*. ArXiv:1905.07830.

Susan Zhang, Stephen Roller, Naman Goyal, Mikel Artetxe, Moya Chen, Shuohui Chen, Christopher Dewan, Mona Diab, Xian Li, Xi Victoria Lin, Todor Miaylov, Myle Ott, Sam Shleifer, Kurt Shuster, Daniel Simig, Punit Singh Koura, Anjali Sridhar, Tianlu Wang, and Luke Zettlemoyer. 2022. **OPT: Open Pre-trained Transformer Language Models**. *arXiv preprint*. ArXiv:2205.01068.

Zhao Zhang, Yangcheng Gao, Jicong Fan, Zhongqiu Zhao, Yi Yang, and Shuicheng Yan. 2025. **SelectQ: Calibration Data Selection for Post-training Quantization**. *Machine Intelligence Research*.

Jiaqi Zhao, Ming Wang, Miao Zhang, Yuzhang Shang, Xuebo Liu, Yaowei Wang, Min Zhang, and Liqiang Nie. 2025. **Benchmarking Post-Training Quantization in LLMs: Comprehensive Taxonomy, Unified Evaluation, and Comparative Analysis**. *arXiv preprint*. ArXiv:2502.13178.

Zifan Zheng, Yezhaohui Wang, Yuxin Huang, Shichao Song, Mingchuan Yang, Bo Tang, Feiyu Xiong, and Zhiyu Li. 2024. **Attention Heads of Large Language Models: A Survey**. *arXiv preprint*. ArXiv:2409.03752.

Xunyu Zhu, Jian Li, Yong Liu, Can Ma, and Weiping Wang. 2024. **A Survey on Model Compression for Large Language Models**. *Transactions of the Association for Computational Linguistics*, 12:1556–1577.

A Experimental Setup

Models, Quantization, and Parameters. Our primary analysis focuses on the Open Pre-trained Transformer (OPT) model family (Zhang et al., 2022), spanning a range of sizes from 125 million to 13 billion parameters (specifically, 125M, 350M, 1.3B, 2.7B, 6.7B, and 13B). For these models, we employ the typical GPTQ (Frantar et al., 2023) as the principal PTQ method. We systematically vary four key parameters: 1) Model Size (N), as listed above; 2) Nominal Bit-width (W_{base}) for weights, exploring 2, 3, 4, and 8 bits; 3) Calibration Set Size (C_b), with 8, 128, 1024, and 4096 samples; and 4) Group Size (G), using values of 32, 64, 128, and 1024. This results in 384 unique PTQ configurations for our main experiments.

To assess generalizability, we also conduct experiments using GPTQ on the LLaMA2 7B and 13B models (Touvron et al., 2023) to selected OPT models (1.3B, 6.7B, 13B) with 2,8 bits quantization.

Calibration Data. For GPTQ experiments, calibration data consists of randomly sampled sequences from the Wikitext2 dataset (Merity et al., 2016). When varying C_b , subsets of the specified sizes are drawn from this pool. Crucially, no calibration data is sourced from our downstream benchmark datasets to prevent data leakage and ensure unbiased evaluation.

Benchmark Tasks and Metrics. We evaluate two primary knowledge capabilities defined in Sec. 3.1. All evaluations are performed in a zero-shot setting.

For **Knowledge Memorization**, we use the LAMA probe (Petroni et al., 2019), specifically its ConceptNet and SQuAD subsets, measuring performance with Pass@1 (P@1) to assess factual recall.

For **Knowledge Utilization**, we employ a suite of commonsense reasoning and question-answering benchmarks: Hellaswag (Zellers et al., 2019), Winogrande (SakaguchiKeisuke et al., 2021), and the AI2 Reasoning Challenge (ARC, including Easy and Challenge subsets) (Clark et al., 2018). Performance is measured by accuracy on each, and we also compute a composite "Knowledge Utilization Score" by averaging accuracies across these three benchmarks.

Implementation Details. Experiments are conducted using the Hugging Face Transformers library (Wolf et al., 2020). GPTQ is implemented

via the AutoGPTQ library (contributors, 2024). Consistent hyperparameters for the quantization algorithms (e.g., dampening factor for GPTQ) are maintained across comparable runs, except for the variables under investigation.

B Task-Stratified Scaling Laws: Memorization vs. Utilization on LLaMA2

To assess the generalizability of our findings, we apply our four-variable scaling law to LLaMA2 models across the two defined task categories, with results presented in Table 3. The scaling law demonstrates a high goodness of fit (Adj. R^2) for both knowledge memorization and utilization tasks on LLaMA2 models. Consistent with our primary findings on OPT models, the relative magnitudes of the fitted coefficients for LLaMA2 reveal that knowledge memorization is markedly more sensitive to variations in effective bit-width (B_{eff}), calibration set size (C_b), and model size (N), while knowledge utilization exhibits greater robustness. The fitted coefficient for group size (G) is a small positive value; this can be understood as the performance benefits from smaller G values being primarily captured through the corresponding increase in B_{eff} , as defined in our scaling law framework. These results on LLaMA2 thereby affirm the broader applicability of our task-stratified scaling laws.

Tasks	C	$\alpha(N)$	$\beta(C_b)$	$\gamma(G)$	$\delta(B_{eff})$	Adj. R^2
General	2.07×10^{-2}	0.0996	0.0270	0.0066	0.7266	0.98
Mem.	1.38×10^{-3}	0.1118	0.0330	0.0051	1.7315	0.91
Util.	3.52×10^{-2}	0.0898	0.0232	0.0095	0.6568	0.98

Table 3: Fitted parameters of $Acc \approx C \times N^\alpha \times [\log_2(C_b)]^\beta \times G^\gamma \times [\log_2(B_{eff})]^\delta$ on multiple LLaMA2 model sizes and task categories.

C Definition of R^2

The coefficient of determination, denoted as R^2 , quantifies the proportion of variance in the dependent variable that is captured by the model. It is defined as:

$$R^2 = 1 - \frac{\sum_{i=1}^n (y_i - \hat{y}_i)^2}{\sum_{i=1}^n (y_i - \bar{y})^2}, \quad (3)$$

where y_i is the true value, \hat{y}_i is the model prediction, and \bar{y} is the empirical mean of the true values. A higher R^2 indicates better explanatory power of the model, with $R^2 = 1$ corresponding to a perfect fit.

Group Size	$B_{eff}(W_{base} = 2)$	$B_{eff}(W_{base} = 3)$	$B_{eff}(W_{base} = 4)$	$B_{eff}(W_{base} = 8)$
16	3.13	4.19	5.25	9.50
32	2.56	3.59	4.63	8.75
64	2.28	3.30	4.31	8.38
128	2.14	3.15	4.16	8.19
256	2.07	3.07	4.08	8.09
512	2.04	3.04	4.04	8.05
1024	2.02	3.02	4.02	8.02

Table 4: Effective bit-width (B_{eff}) for different group sizes and base weight bit-widths (W_{base}).

D Effective Bit-width (B_{eff}) Values

We further provide a detailed table of Effective Bit-width (B_{eff}) values calculated for various combinations of nominal bit-width (W_{base}) and group size (G). As shown in Table 4, these values correspond to the conceptual data visualized in the main text, which illustrates the impact of these parameters on B_{eff} .